

University of Groningen

## Spin Gap and Antiferromagnetic Correlations in the Kondo Insulator CeNiSn

Mason, T.E.; Aeppli, G.; Ramirez, A.P.; Clausen, K.N.; Broholm, C.; Stücheli, N.; Bucher, E.; Palstra, T.T.M.

*Published in:*  
Physical Review Letters

*DOI:*  
[10.1103/PhysRevLett.69.490](https://doi.org/10.1103/PhysRevLett.69.490)

**IMPORTANT NOTE: You are advised to consult the publisher's version (publisher's PDF) if you wish to cite from it. Please check the document version below.**

*Document Version*  
Publisher's PDF, also known as Version of record

*Publication date:*  
1992

[Link to publication in University of Groningen/UMCG research database](#)

*Citation for published version (APA):*

Mason, T. E., Aeppli, G., Ramirez, A. P., Clausen, K. N., Broholm, C., Stücheli, N., Bucher, E., & Palstra, T. M. (1992). Spin Gap and Antiferromagnetic Correlations in the Kondo Insulator CeNiSn. *Physical Review Letters*, 69(3). <https://doi.org/10.1103/PhysRevLett.69.490>

### Copyright

Other than for strictly personal use, it is not permitted to download or to forward/distribute the text or part of it without the consent of the author(s) and/or copyright holder(s), unless the work is under an open content license (like Creative Commons).

The publication may also be distributed here under the terms of Article 25fa of the Dutch Copyright Act, indicated by the "Taverne" license. More information can be found on the University of Groningen website: <https://www.rug.nl/library/open-access/self-archiving-pure/taverne-amendment>.

### Take-down policy

If you believe that this document breaches copyright please contact us providing details, and we will remove access to the work immediately and investigate your claim.

*Downloaded from the University of Groningen/UMCG research database (Pure): <http://www.rug.nl/research/portal>. For technical reasons the number of authors shown on this cover page is limited to 10 maximum.*

## Spin Gap and Antiferromagnetic Correlations in the Kondo Insulator CeNiSn

T. E. Mason,<sup>(1),(2)</sup> G. Aeppli,<sup>(1)</sup> A. P. Ramirez,<sup>(1)</sup> K. N. Clausen,<sup>(2)</sup> C. Broholm,<sup>(3)</sup> N. Stücheli,<sup>(5)</sup>  
E. Bucher,<sup>(1),(4)</sup> and T. T. M. Palstra<sup>(1)</sup>

<sup>(1)</sup>*AT&T Bell Laboratories, Murray Hill, New Jersey 07974*

<sup>(2)</sup>*Risø National Laboratory, 4000 Roskilde, Denmark*

<sup>(3)</sup>*The Johns Hopkins University, Baltimore, Maryland 21218*

<sup>(4)</sup>*University of Konstanz, 7750 Konstanz, West Germany*

<sup>(5)</sup>*Eidgenössische Technische Hochschule, Zurich, Switzerland*

(Received 2 March 1992)

Neutron scattering measurements show that the crossover (at  $T \lesssim 10$  K) from metallic heavy-fermion to semiconducting behavior coincides with the formation of a gap in the magnetic excitation spectrum of CeNiSn. In contrast to the simple band picture of an insulator, the gap is well defined only at particular values of the momentum transfer  $Q$ . While substantial antiferromagnetic correlations in the  $a$ - $c$  plane characterize the low- $T$  state, the corresponding zero-frequency response function is  $Q$  independent.

PACS numbers: 71.28.+d, 72.15.Qm, 75.20.Hr

Heavy-fermion materials, which are typically Ce and U compounds characterized by large Sommerfeld constants, exhibit all possible metallic ground states, ranging from Pauli paramagnetic to superconducting. Recently, it has become apparent that they can also display semiconducting properties at low temperatures [1-4]. Because antiferromagnetic correlations are at the heart of the phenomenon of heavy-fermion metals [5,6], it is important to examine the magnetic correlations in a heavy-fermion semiconductor. We have therefore performed neutron scattering measurements on single crystals of such a material, CeNiSn [7]. The principal finding is that with decreasing  $T$ , the magnetic response evolves smoothly from the wave-vector- ( $Q$ -) independent continuum associated with heavy-fermion metals above their coherence temperatures to spectra dominated by excitations beyond a gap which is well defined only near particular values of  $Q$ . Furthermore, in contrast to what happens in all other rare-earth and actinide compounds with a  $Q$ -dependent response at finite frequencies, the magnetic interactions, as probed in the [010] plane in the present experiment, appear to vanish at zero frequency.

CeNiSn crystallizes in the orthorhombic  $\epsilon$ -TiNiSn structure with room-temperature lattice parameters  $a = 7.523$  Å,  $b = 4.592$  Å, and  $c = 7.561$  Å [8]. We fabricated single crystals 5-6 mm in diameter and 4 cm long parallel to  $\mathbf{b}$  by electron beam zone refinement of polycrystalline ingots of CeNiSn. Both polycrystalline and single-crystal samples were annealed in vacuum ( $P < 10^{-7}$  torr) at 750°C for 200 h, followed by a cool-down of 1.5°/h to 500°C, where the furnace was shut off.

Figures 1(a) and 1(b) show bulk properties of our samples and also demonstrate why CeNiSn has been considered a heavy-fermion semiconductor. As for samples prepared by other groups [2,3], extrapolation of  $C/T$  measured for  $T > 5$  K to 0 K gives a Sommerfeld constant of 200 mJ/moleK<sup>2</sup>, corresponding to a band of moderately heavy carriers. In the region ( $T > 5$  K) where the magnetic contribution to  $C/T$  is essentially

constant, the resistivity  $\rho(T)$  behaves much as it does in other anisotropic heavy-fermion compounds [9] near their coherence temperatures: It decreases initially with  $T$  for certain directions and is essentially  $T$  independent for others. More unusual behavior sets in below 5 K, where  $C/T$  is substantially reduced and  $\rho(T)$  increases dramatically. Hall effect measurements [10] confirm that these effects are due to a loss of carriers, as would occur near a metal-insulator transition. For CeNiSn, in contrast to Ce<sub>3</sub>Bi<sub>4</sub>Pt<sub>3</sub> [1], the loss of carriers is not complete, as suggested by the finite value of  $C/T$  as  $T \rightarrow 0$  and the downturn in  $\rho(T)$  for  $T < 1$  K. Because the carrier densities given by the Hall effect data for 1.3 K are low ( $< 10^{-2}$  carrier per formula unit), the effective mass of the remaining carriers is extremely large. Below 5 K,  $\rho(T)$  is well represented [solid line in 1(b)] by the resistivity for a metal in parallel with that for a semiconductor. More precisely,

$$\rho^{-1}(T) \cong \rho_M^{-1} + \rho_s^{-1} = \sigma_M [1 + (T/T_0)^2]^{-1} + \sigma_s \exp(-\frac{1}{2} E_g/k_B T), \quad (1)$$

where the parameters  $T_0 = 1.4$  K and  $E_g = 6.8$  K.

For our neutron scattering experiments at Risø National Laboratory, we mounted our CeNiSn so that its [010] zone coincided with the horizontal scattering planes of the spectrometers. Figure 2 shows the  $Q$  dependence of the scattering corresponding to an integral of  $S(Q, \omega)$  over energies  $\hbar\omega$  between 1.75 and 5.5 meV at  $T = 1.4$  and 13 K. It is clear from the figure that short-range correlations develop as the temperature is lowered. They are most strongly peaked near (0,0,1), a forbidden nuclear reflection, and are thus antiferromagnetic in nature. The scattering for  $\mathbf{Q} \parallel \mathbf{a}^*$  is not modulated and weaker (the dash-dotted line in Fig. 2 represents its level). In view of the dipole selection rule for magnetic neutron scattering, this indicates that the magnetic fluctuations are primarily polarized along the  $a$  axis which, from the bulk susceptibility data [3], is also the easy magnetic

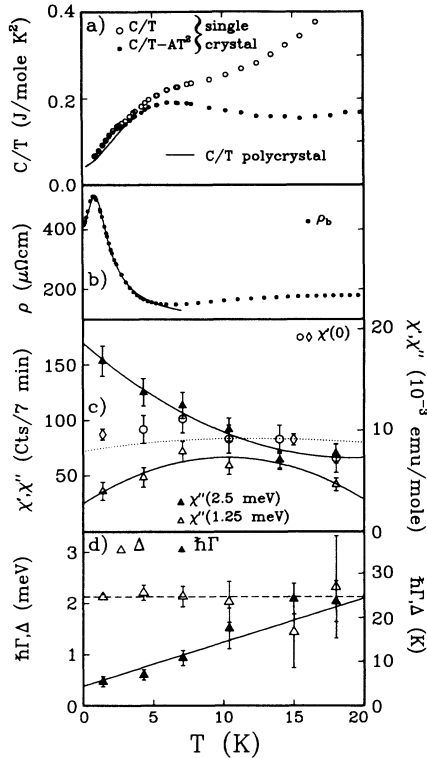


FIG. 1. (a) Ratio of specific heat, uncorrected and corrected for a Debye term  $AT^3$  ( $A=0.792 \times 10^{-3}$  J/mole  $K^4$ ), to temperature. The small bulge at 2 K in the single-crystal data (open and solid circles) is not present for the annealed polycrystal (solid line), where phase separation is less likely. We suspect that the bulge, which accounts for an entropy loss of  $8 \times 10^{-3} R \ln 2$  is due to the antiferromagnetic phase transition [19] in a small amount of  $CeNi_2Sn_2$  produced during zone refinement. (b) Resistivity along  $b$  axis. Solid curve corresponds to Eq. (1) in text with parameters  $\sigma_M=0.0023$  ( $\mu\Omega\text{cm}$ ) $^{-1}$ ,  $T_0=1.41$  K,  $\sigma_s=0.012$  ( $\mu\Omega\text{cm}$ ) $^{-1}$ , and  $E_g=6.8$  K obtained from fits to  $\rho_b(T)$ . (c)  $\chi''$  at  $Q=(0,0,1.2)$  for  $\hbar\omega=2.5$  meV and  $\hbar\omega=1.25$  meV. Also shown (in same units) is  $\chi'(Q,0)$  obtained from the Kramers-Kronig transform of measured  $\chi''(Q,\omega)$ . Diamonds correspond to high-resolution data. Solid curves are guides to eye. Dotted line corresponds to bulk ( $Q=0$ ) susceptibility measured along the  $a$  axis (from Ref. [3]). (d)  $\Delta$  and  $\hbar\Gamma$  extracted from fits described in text.

axis.

We have carried out more detailed constant- $Q$  measurements (Fig. 3) of the spin fluctuation spectrum using higher-resolution [full width at half maximum (FWHM), 0.25 meV] triple-axis spectroscopy. For  $Q$  near (0,0,1) (top panel of Fig. 3), where the energy-integrated spectrum (see Fig. 2) peaks, there is little scattering at low  $T$  for  $\hbar\omega \leq 1.75$  meV. Above 1.75 meV,  $S(Q,\omega)$  rises rapidly to a maximum at 2.5 meV and then decays rather slowly. The second panel shows the energy dependence further away from (0,0,1), at (0.36,0,1.2). The sharp feature visible at (0,0,1.2) has broadened considerably and decreased in intensity. For  $Q$  along  $a^*$  (bottom

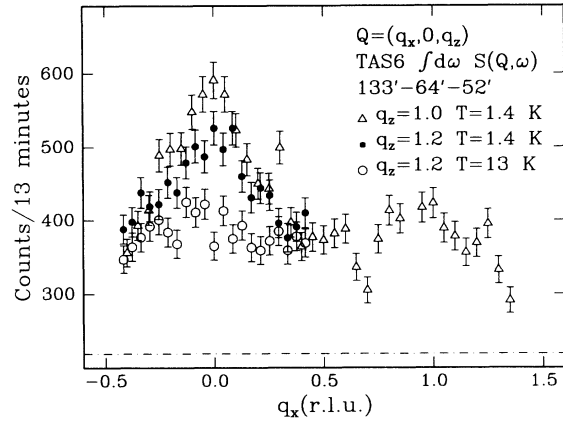


FIG. 2. Scans as function of  $Q$  probing integral of  $S(Q,\omega)$  from 1.75 to 5.5 meV. Dash-dotted line represents  $Q$ -independent scattering (including nonmagnetic background) measured for  $Q||a^*$ .

panel), there is only a very weak quasielastic signal which is of the same size as the response below 1.75 meV at  $Q=(0,0,1.2)$ . Indeed, this contribution appears at all measured  $Q$ 's indicating that it is isotropic in the [010] plane. The absence of the gapped signal for  $Q||a^*$  shows

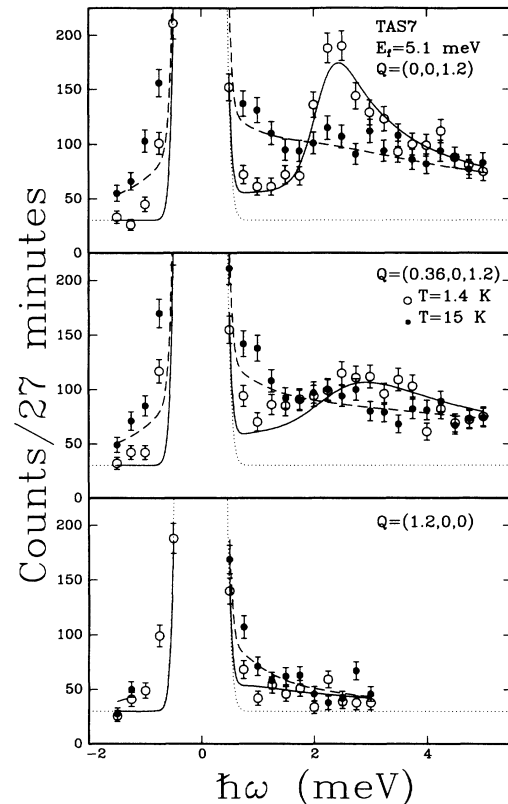


FIG. 3. Constant- $Q$  scans at  $T=1.4$  K ( $\circ$ ) and  $T=15$  K ( $\bullet$ ). The dotted lines are the flat and incoherent elastic contributions to the background. Solid lines are obtained from fits described in text.

that it, like the antiferromagnetic correlations in Fig. 2, is due to spin excitations polarized along  $\mathbf{a}^* \parallel \mathbf{a}$ . At 15 K (solid circles), a large part of the spectral weight above the gap in the Ising-like fluctuations for  $T=1.4$  K has shifted to lower frequency, resulting in a quasielastic response with a  $Q$ -independent damping similar to that seen both in conventional Ce heavy-fermion systems at high  $T$  [6], and also in CeNiSn powder at 20 K [11].

In addition to the high-resolution measurements shown in Fig. 3, we performed an extensive survey of  $S(Q, \omega)$  with an energy resolution of 1 meV (FWHM). Figure 1(c) shows the temperature dependence of  $\chi''$  [obtained by correcting the raw data for background and removing the trivial  $n(\omega)+1$  factor] for  $\hbar\omega=1.25$  meV, below the energy of the gap that appears at low  $T$ , and for  $\hbar\omega=2.5$  meV, where the low- $T$  response is largest. Opposing tendencies which correlate with gap formation become obvious in the  $T$ -dependent  $\chi''$  for the two  $\omega$ 's only for  $T \leq 7.5$  K, which is also where the crossover to semiconducting behavior occurs in  $\rho$  and  $C/T$ .

Our experiments show that on reducing  $T$ , there is a growth of magnetic correlations as the quasiparticle states become sufficiently coherent for  $\chi''(Q, \omega)$  to display a spin gap. Thus, CeNiSn is similar to heavy-fermion metals, where  $\chi''(Q, \omega)$  becomes strongly  $Q$  dependent below the coherence temperature deduced from transport measurements [6]. For the metals, the concomitant growth in magnetic correlations (and appearance of "metamagnetism" in bulk thermodynamic properties [12]) can be described in terms of a Ruderman-Kittel-Kasuya-Yosida coupling [6,7]  $J(Q)$ . The coupling increases as  $T$  is reduced to enter the coherent Fermi-liquid regime, and manifests itself in the zero-frequency (real) susceptibility  $\chi'(Q, 0)$ , which, in the random-phase approximation, can be written as  $\chi_0/[1 - \chi_0 J(Q)]$ , where  $\chi_0$  is the single-ion susceptibility. To determine whether CeNiSn exhibits the same phenomenon, we have performed numerical Kramers-Kronig transforms of our constant- $Q$  and  $-T$  spectra to obtain the easy-axis ( $a$ ) susceptibility. The open circles (low-resolution data) and diamonds (high-resolution data) in Figs. 1(c) and 4 represent the outcome of the analysis. The principal result is that to within experimental error,  $\chi'(Q, 0)$  is  $Q$  independent over the range of wave vectors and temperatures probed. Conversion of the magnetic intensities into absolute units [13] shows that  $\chi'(Q, 0)$  is also indistinguishable from the measured [3] bulk ( $Q=0$ ) susceptibility, also shown in the figures. Thus, as  $\omega \rightarrow 0$ , the magnetic moments in CeNiSn are effectively noninteracting in the  $a$ - $c$  plane, even though  $\chi''(Q, \omega)$  depends strongly on  $Q$ . This is extraordinary because in all other rare-earth and actinide materials with  $Q$ -dependent  $\chi''(Q, \omega)$ , which range from magnets [14] like Ho to heavy-fermion superconductors and paramagnets like UPt<sub>3</sub> and CeCu<sub>6</sub> [6,7],  $\chi'(Q, 0)$  is always a nontrivial function of  $Q$  at low  $T$ . Among transition metal compounds, there is one, FeSi,

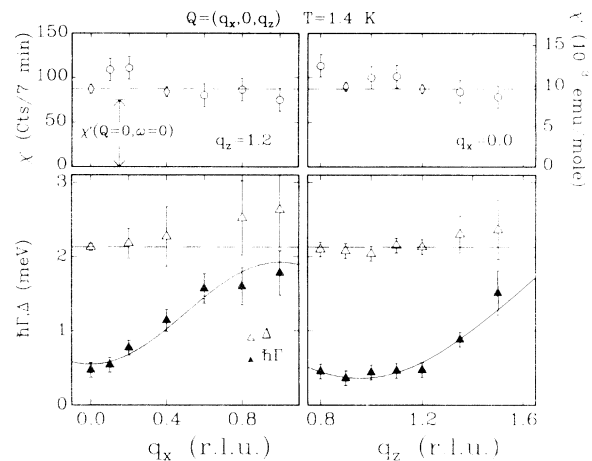


FIG. 4.  $\chi'(Q, 0)$  obtained from the numerical Kramers-Kronig transform and parameters  $\Delta$  and  $\hbar\Gamma$  given by fits of Eq. (2) to constant- $Q$  scans. Diamonds correspond to high-resolution data.

which simultaneously displays  $Q$ -independent  $\chi'(Q, 0)$  and strongly  $Q$ -dependent  $\chi''(Q, \omega)$  [15]. However, we believe that it is no coincidence that FeSi is also a small-gap semiconductor [16], with unusual  $T$ -dependent properties attributed to moment formation at high  $T$ .

One of the most striking features of the low-temperature data in the first panel of Fig. 3 is the asymmetry about the peak at  $\sim 2.5$  meV, which is not consistent with the slight asymmetry present in the quasielastic or inelastic Lorentzian line shapes usually employed to describe magnetic fluctuations in Ce heavy-fermion systems [6,7]. Indeed, the spectrum resembles more a broadened version of the form  $\chi'' \sim \omega \theta(\omega^2 - \Delta^2)(\omega^2 - \Delta^2)^{-\alpha}$  ( $\theta$  is the unit step function), where the singularity at  $\omega = \pm \Delta$  could appear in the Lindhard function derived from a band-structure calculation [17]. On the other hand, for large  $T$ , the quasielastic form,  $\chi'' \sim \omega \Gamma / (\omega^2 + \Gamma^2)$ , typical of Kondo metals, does describe the data. A function which interpolates between the two simple forms (for simplicity, we consider only  $\alpha=1$ ) is

$$\chi''(Q, \omega) = \chi_0 |\epsilon(Q)| \omega \{ \text{Re}[\omega - \epsilon(Q)]^{-1/2} \}^2, \quad (2)$$

where

$$\epsilon(Q) = \hbar^{-1} \Delta(Q) + i\Gamma(Q).$$

Thus, we have parametrized our data using a magnetic response function which is a sum of the form above and a  $Q$ -independent quasielastic term (with  $\hbar\Gamma_0=0.8$  meV) to account for the Ising-like and isotropic fluctuations, respectively. These terms correspond to the semiconducting and metallic contributions to the conductivity in our parallel-resistor model, Eq. (1). Figure 4 shows how the values of  $\Delta$  and  $\hbar\Gamma$  obtained from fits to our spectra vary with  $Q$ . The damping  $\Gamma$  is clearly smallest for  $Q$  near

(0,0,1). As  $\Gamma$  increases when  $Q$  deviates from (0,0,1),  $\hbar\Gamma/\Delta$  rises towards unity. Here the excitations responsible for  $\chi''(Q,\omega)$  are overdamped, so that  $\Gamma$  and  $\Delta$  cannot be simultaneously determined with great accuracy. The gap  $\Delta$  is larger than the effective transport gap  $E_g$  [Eq. (1)] presumably because of states with energies below  $\Delta$ , associated with the substantial dampings measured at most  $Q$ 's. It is also essentially  $Q$  independent, implying that the variation of the damping  $\Gamma$  with  $Q$  accounts for the entire  $Q$  dependence of  $\chi''(Q,\omega)$ , in the portion of the [010] plane which we have probed. In contrast, for all other (except possibly TmSe) rare-earth [14] compounds where single-crystal neutron spectroscopy has yielded sharp magnetic peaks at  $\omega \neq 0$ , the dispersion relation for the excitations and not the  $Q$  dependence of their lifetimes dominates the  $Q$  dependence of  $\chi''(Q,\omega)$ . TmSe deserves special mention because it is a semiconducting antiferromagnet which shares with CeNiSn the development at low  $T$  of an inelastic feature with decidedly modest dispersion [18]. However, in contrast to what occurs in CeNiSn, the feature appears together with a quasielastic peak, and is not correlated with an obvious metal-insulator crossover.

Figure 1(d) shows how  $\Delta$  and  $\hbar\Gamma$  depend on  $T$  for  $Q=(0,0,1.2)$ . For higher  $T$ , the spectra begin to resemble those of conventional Kondo metals, so that  $\Delta$  and  $\Gamma$  become correlated. Even so, it is clear that the gap parameter  $\Delta$  changes little, if at all, with  $T < 20$  K. We conclude that the *apparent* (see Fig. 3) collapse of the gap on warming is primarily due to a reduction in the lifetime of the excitations near the fixed gap frequency. The decay rate  $\hbar\Gamma$  rises with  $T$  in rough accord with the expression  $\hbar\Gamma = k_B T_0 + k_B T$  [solid line in Fig. 1(d)], where  $k_B T_0 = 0.4$  meV. That temperature is the scale for the broadening of the excitations suggests that interactions are effectively absent, as also concluded from the  $Q$  independence of  $\chi'(Q,0)$ . This result, which we believe to be independent of the form used to parametrize the data, is not what occurs in ordinary semiconductors where intrinsic carrier lifetimes are  $\gg \hbar(k_B T)^{-1}$ , but might happen in a semiconductor where electron-hole pairs consist of stationary Kondo spins and mobile carriers scattering from the spins.

In conclusion, we have shown that the appearance of a spin gap and strongly  $Q$ -dependent finite-frequency response characterizes the crossover to coherence in the heavy-fermion semiconductor CeNiSn. That the gap is well defined only at particular values of  $Q$  shows that CeNiSn is not simply a semiconductor with heavy quasiparticles in the conduction and valence bands.

We are grateful to E. Abrahams, Z. Fisk, P. Littlewood, A. Millis, P. Riseborough, A. Severing, J. Thompson, T. Takabatake, and C. M. Varma for useful discussions and preprints and J. Als-Nielsen and J. Kjems for their encouragement and hospitality at Risø where this work was funded by the Danish Natural Science Research Council. T.E.M. acknowledges the financial support of NSERC.

- 
- [1] M. F. Hundley *et al.*, Phys. Rev. B **42**, 6842 (1990).
  - [2] F. G. Aliev *et al.*, Pis'ma Zh. Eksp. Teor. Fiz. **48**, 630 (1988) [JETP Lett. **48**, 581 (1988)].
  - [3] T. Takabatake *et al.*, Phys. Rev. B **41**, 9607 (1990).
  - [4] A. Severing *et al.*, Phys. Rev. B **44**, 6832 (1991).
  - [5] *Physical Phenomena at High Magnetic Fields, Proceedings*, edited by E. Manousakis *et al.* (Addison-Wesley, Redwood City, 1992).
  - [6] See, e.g., G. Aeppli, in *Theoretical and Experimental Aspects of Valence Fluctuations and Heavy Fermions*, edited by L. C. Gupta and S. K. Malik (Plenum, New York, 1987); and C. M. Varma, in *Physical Phenomena at High Magnetic Fields, Proceedings* (Ref. [5]).
  - [7] In Ref. [5], G. Aeppli, E. Bucher, and T. Mason, give a preliminary account of the spin-gap formation in CeNiSn.
  - [8] R. V. Skolozdra, O. E. Koretshraya, and Yu. K. Gorelenko, Inorg. Mater. **20**, 604 (1984).
  - [9] See, e.g., B. Batlogg *et al.*, J. Appl. Phys. **55**, 2001 (1984).
  - [10] T. Takabatake *et al.* (to be published).
  - [11] M. Kohgi *et al.* (to be published).
  - [12] See, e.g., P. H. Frings and J. J. M. Franse, Phys. Rev. B **31**, 4355 (1985).
  - [13] We applied the procedure of O. Steinsvoll *et al.* [Phys. Rev. B **30**, 2377 (1984)] using the transverse acoustic phonon at  $Q=(2,0,\pm 0.16)$  and  $\hbar\omega=2.5$  meV.
  - [14] For a review of the magnetic properties of rare earths, see J. Jensen and A. Mackintosh, *Rare Earth Magnetism* (Oxford Univ. Press, Oxford, 1991).
  - [15] G. Shirane *et al.*, Phys. Rev. Lett. **59**, 351 (1987); K. Tajima *et al.*, Phys. Rev. B **38**, 6954 (1988).
  - [16] V. Jaccarino *et al.*, Phys. Rev. **150**, 476 (1967).
  - [17] P. Riseborough (to be published) shows that such singularities are also found when many-body effects are accounted for in the mean-field slave boson [see also A. Millis, in *Physical Phenomena at High Magnetic Fields, Proceedings* (Ref. [5])] approximation.
  - [18] S. M. Shapiro and B. H. Grier, Phys. Rev. B **25**, 1457 (1982); A. J. Fedro and S. K. Sinha, in *Valence Fluctuations in Solids*, edited by L. M. Falikov, W. Hanke, and M. B. Maple (North-Holland, New York, 1987).
  - [19] T. Takabatake *et al.*, J. Magn. Magn. Mater. **90-91**, 474 (1990).